An image registration algorithm based on phase correlation and the classical Lucas–Kanade technique

Article *in* Signal Image and Video Processing · May 2017

DOI: 10.1007/s11760-017-1089-4

CITATIONS
8

READS
357

4 authors, including:

Jamal Riffi
Sidi Mohamed Ben Abdellah University
27 PUBLICATIONS **102** CITATIONS

SEE PROFILE

M. A. Mahraz
Sidi Mohamed Ben Abdellah University
15 PUBLICATIONS **93** CITATIONS

SEE PROFILE

H. Tairi
Sidi Mohamed Ben Abdellah University
173 PUBLICATIONS **584** CITATIONS

SEE PROFILE

An image registration algorithm based on phase correlation and the classical Lucas–Kanade technique

Youssef Douini, Jamal Riffi, Adnane Mohamed Mahraz & Hamid Tairi

Signal, Image and Video Processing

ISSN 1863-1703

SIViP
DOI 10.1007/s11760-017-1089-4

Springer

SIViP
DOI 10.1007/s11760-017-1089-4

ORIGINAL PAPER

An image registration algorithm based on phase correlation and the classical Lucas–Kanade technique

Youssef Douini[1] · **Jamal Riffi**[1] · **Adnane Mohamed Mahraz**[1] · **Hamid Tairi**[1]

Received: 19 July 2016 / Revised: 23 March 2017 / Accepted: 27 March 2017

Abstract Image registration is defined as an important process in image processing in order to align two or more images. A new image registration algorithm for translated and rotated pairs of 2D images is presented in order to achieve subpixel accuracy and spend a small fraction of computation time. To achieve the accurate rotation estimation, we propose a two-step method. The first step uses the Fourier Mellin Transform and phase correlation technique to get the large rotation, then the second one uses the Fourier Mellin Transform combined with an enhance Lucas–Kanade technique to estimate the accurate rotation. For the subpixel translation estimation, the proposed algorithm suggests an improved Hanning window as a preprocessing task to reduce the noise in images then achieves a subpixel registration in two steps. The first step uses the spatial domain approach which consists of locating the peak of the cross-correlation surface, while the second uses the frequency domain approach, based on low-frequency (aliasing-free part) of aliased images. Experimental results presented in this work show that the proposed algorithm reduces the computational complexities with a better accuracy compared to other subpixel registration algorithms.

✉ Youssef Douini
youssef.douini@usmba.ac.ma

Jamal Riffi
riffi.jamal@gmail.com

Adnane Mohamed Mahraz
adnane_1@yahoo.fr

Hamid Tairi
htairi@yahoo.fr

[1] Department of Computer Science, Sidi Mohamed Ben Abdellah University, Fez, Morocco

Keywords Image registration · Fourier Mellin Transform · Phase correlation · Lucas–Kanade technique · Hanning window · Aliased images

1 Introduction

The rigid image registration technique has been a hot research field of image processing. It refers to the process of aligning two images (or more) of the same target in space. Although pixel level registration may be sufficient in many applications, but some important problems like medical imaging, biometrics, image mosaicking, video stabilization, and others have introduced the requirement of subpixel registration. Numerous methods and techniques have been proposed for these different applications [1,2]. These techniques can be classified into two categories: feature-based and area-based techniques [3]. The process of image registration is mainly composed of the three elements:

- A transformation space: linear [4], elastic [5,6], etc.;
- Similarity criterion: sum of squared differences [7], correlation coefficient [8], correlation ratio [9], mutual information [10], etc.;
- An optimization algorithm: Powell method, stochastic search, etc.;

In recent years, the most popular techniques for subpixel image registration use the peak location of the cross-correlation surface to register or align the images, due to its remarkable accuracy and robustness to uniform variations of illumination and signal noise in images [11–14]. These techniques can be classified in spatial domain approaches and frequency domain approaches.

The idea of spatial domain approaches is to calculate an up-sampled version of cross-correlation between two images using zero-padded Fast Fourier Transform

Published online: 02 May 2017

(FFT). This approach provides highly accurate and robust results; however, its great complexity and huge memory requirements rend it unrealistic, especially for large-size images. The computation complexity of this method is $o\{MNk\left[\log_2(kM) + k\log_2(kM)\right]$, where k is the up-sampling factor, and M and N are the image dimensions. To overcome these drawbacks, Guizar-Sicairos [14] proposed a new algorithm that uses Discrete Fourier Transform (DFT) matrix-multiplication to compute the cross-correlation surface between images. We refer to it as single-step DFT approach (SSDFT). This method reduces computation time and memory requirements. In addition, it does not ignore sacrificing the accuracy obtained by the traditional method which uses zero-padded FFT.

To overcome the limitations of spatial domain techniques, many researchers looked for a direct solution in frequency domain based on the Fourier shift theorem. These methods investigate the effects of aliasing and proposed a new algorithm in which the translational parameters are directly estimated in Fourier domain. Several algorithms have been proposed by [15–18].

In this article, in order to achieve the accurate rotation estimation, we propose a two-step method. The first step uses the Fourier Mellin Transform and phase correlation technique to get the large rotation, while the second one uses the Fourier Mellin Transform combined with an enhance Lucas–Kanade technique to estimate the accurate rotation. For the subpixel translation estimation, a meta-algorithm was proposed by combining the advantages of both approaches: spatial and frequency domain. First, an improved Hanning window which reduces the noise in images was applied, then the shift parameters were estimated in two steps: the first step uses a phase correlation registration algorithm to find a translation that registers the two images to the nearest integral pixel coordinates by using a down-sampled Fourier Transform of the two images, then the subpixel registration is directly estimated in frequency domain through least-squares technique. In the experiments, we found that the proposed algorithm reduces the computational complexities with a better accuracy compared to other subpixel registration algorithms.

The paper is organized as follows: Sect. 2 describes briefly spatial domain approaches used in image registration. The frequency domain approaches are described in Sect. 3 and the proposed approach in Sect. 4. In Sects. 5 and 6, simulations and results are compared and analyzed to make the final conclusion.

2 Spatial domain approaches

2.1 Phase correlation method

The original phase correlation method proposed by Kuglin and Hines [11] is known to identify integer pixel displacement between images. It is based on the well-known Fourier shift property: a shift in the spatial domain of two images results as a linear phase difference in the frequency domain of the Fourier Transforms (FT).

Given two 2D functions $f(x, y)$ and $g(x, y)$ representing two images related by a simple translational shift a in horizontal and b in vertical directions, f and g are related by the following transformation:

$$f(x, y) = g(x + a, y + b) \tag{1}$$

where $[x, y] \in R^2$ and $[a, b] \in R^2$. The normalized cross-power spectrum between F and G is defined as following:

$$C(u, v) = \frac{F(u, v)\, G^*(u, v)}{||F(u, v)\, G^*(u, v)||} = \mathrm{e}^{-2i\pi\left(\frac{ua}{M} + \frac{vb}{N}\right)} \tag{2}$$

M and N stand for the image dimensions, while $F(x, y)$ and $G(x, y)$ represent the DFT of images, * denotes complex conjugation. The inversed Fourier Transform (IFT) of $C(x, y)$ is a Dirac delta function centered in $(-a, -b)$:

$$\mathrm{IFT}(C(u, v)) = \delta(x + a, y + b) \tag{3}$$

2.2 SSDFT approach

To get the accurate peak location, the usual approach calculates an up-sampled version of the cross-correlation surface between the two images using Fast Fourier Transform (FFT). The main disadvantages of this approach are the huge waste of memory and time. However, in order to resolve these problems, we used the SSDFT [14] approach which is based on the method of matrix-multiply DFT. This method does not need to zero-padding the Fourier Transform of the both images to obtain an up-sampled version of the phase correlation. Let $f(x, y)$ be the input image and $\in$ the sampling factor. The method of matrix-multiply DFT calculates the up-sampled Fourier Transform of f in a small window u, v (4):

$$\begin{aligned}
&\hat{F}(U, V) = \mathrm{e}^{-2i\pi U x^{\mathrm{T}}} f(x, y)\, \mathrm{e}^{-2i\pi V y^{\mathrm{T}}} \\
&(a)\ U = (u_0, u_1, \ldots, u_{n-1}) \\
&(b)\ V = (v_0, v_1, \ldots, v_{m-1}) \\
&(c)\ x = (x_0, x_1, \ldots, x_{N\times\in-1}) \\
&(d)\ y = (y_0, y_1, \ldots, y_{M\times\in-1})
\end{aligned} \tag{4}$$

where $n \times m$ and $N \times M$ are the dimensions of f and u, v window, respectively.

To refine the estimate parameters, the SSDFT approach uses two steps. The first step finds the initial estimate using the FFT method with up-sampled factor $\in = 2$, and in the second step, an up-sampled version of cross correlation (by

factor $\in$) is computed in a (1.5×1.5) pixel neighborhood of the initial estimate using a matrix-multiplication which calculates the Fourier Transform of some points of sequence mainly by using the properties of the matrix.

3 A frequency domain approaches

The spatial domain approaches are the mostly used methods to estimate the shift parameter based on the calculation of normalized cross-power spectrum (2) between source and reference images sampled by a factor k. This method preserves registration accuracy, but its complexity is dramatically immense. For these reasons, several approaches using the frequently domain instead of the spatial domain had been proposed as described in [15–17,19]. As the magnitude of $C(u, v)$ (2) is normalized to 1, the only variable that remains is the phase difference defined by $\frac{ua}{M} + \frac{vb}{N}$. It is shown that the parameters a and b can be calculated using only Eq. (2) without applying IFT, using just a least-squares fitting (LSF) method or other methods such as technical Quick Maximum Density Power Estimator (QMDPE). Aliasing problem is a potential drawback of these methods, this problem does not occur above the Nyquist frequency, but in below the Nyquist frequency aliasing can occur. Consequently, the aliased spectrum will be different than the original spectrum. So, in the presence of aliasing these methods do not provide a high registration precision. This is due to the difference in frequency between source and reference images. In this case, the relationship between Fourier transforms of the two images can be expressed as follows:

$$G(u, v) = \sum_{-k_1}^{k_1} \sum_{=-k_2}^{-k_2} F(u - k_1 u_s, v - k_2 v_s)\, \mathrm{e}^{-2i\pi\left(\left(\frac{ua}{M} - k_1 u_s\right) + \left(\frac{vb}{N} - k_2 v_s\right)\right)} \tag{5}$$

where $\boldsymbol{u_s}$: sampling frequency in horizontal direction, $\boldsymbol{v_s}$: sampling frequency in vertical direction, $\boldsymbol{k_1}$: overlapping spectrum copies at frequency $\boldsymbol{u}$, $\boldsymbol{k_2}$: overlapping spectrum copies at frequency $\boldsymbol{v}$.

In order to eliminate the aliased frequency components in the registration process, high frequency of the normalized cross-power spectrum should be filtered, and only the lower-frequency part near the origin is conserved [16].

4 The proposed approach

A new algorithm which reduces the required time and memory compared with other algorithms was proposed. The technique achieves subpixel translation and accurate rotation in two steps. The first step detects the accurate rotation, while the second estimates the subpixel translation.

4.1 Rotation estimation

To obtain high-accuracy rotation estimation, we summarize this procedure as follows:

- Step 1: aims to estimate the large rotation between the two images using the principle of phase correlation;
- Step 2: aims to estimate the accurate rotation between the two images;

4.1.1 First step

To achieve the large rotation estimation we propose to use the following steps:

1. Get the magnitude Fourier Transform of the two images which exhibits the rotation, but not translation;
2. Convert the rotation into translation by using the log-polar conversation;
3. Finally, apply the phase correlation technique described in Sect. 2.

The necessary theorem of these steps is:
First step The movement can be described by a function of three variables: the horizontal shift a, vertical shift b, and rotation $\Delta\theta$. Assume we have the reference f image and its translated and rotated image g:

$$g(x) = f(R(x + \Delta x)) \tag{6}$$

With $x = \begin{bmatrix} x \\ y \end{bmatrix}$, $\Delta x = \begin{bmatrix} a \\ b \end{bmatrix}$, $R = \begin{pmatrix} \cos(\Delta\theta) & -\sin(\Delta\theta) \\ \sin(\Delta\theta) & \cos(\Delta\theta) \end{pmatrix}$
In the Fourier domain we have:

$$\begin{aligned} G(w) &= \iint g(x) \mathrm{e}^{-2\pi i w^T x} \mathrm{d}x \\ &= \iint f(R(x + \Delta x))\, \mathrm{e}^{-2\pi i w^T x} \mathrm{d}x \\ &= \mathrm{e}^{2\pi i u^T \Delta x} \iint f\left(Rx'\right) \mathrm{e}^{-2\pi i w^T x'} \mathrm{d}x' \end{aligned} \tag{7}$$

With $x' = x + \Delta x$ and G the Fourier Transform of g.so, the amplitude of G is:

$$\begin{aligned} |G(w)| &= \left| \mathrm{e}^{2\pi i u^T \Delta x} \iint f\left(Rx'\right) \mathrm{e}^{-2\pi i w^T x'} \mathrm{d}x' \right| \\ &= \left| \iint f\left(Rx'\right) \mathrm{e}^{-2\pi i w^T x'} \mathrm{d}x' \right| \\ &= |F(Rw)| \end{aligned} \tag{8}$$

Second step The representation of $|F(w)|$ and $|G(w)|$ in polar coordinates is:

$$|F(w)| = \hat{F}(\ln\rho, \theta) = \hat{F}(\hat{\rho}, \theta)$$
$$|G(w)| = \hat{G}(\ln\rho, \theta) = \hat{G}(\hat{\rho}, \theta) \quad (9)$$

where ρ is the polar radius and $\hat{\rho} = \ln\rho$. So, we can rewrite Eq. (8) by:

$$\hat{G}(\hat{\rho}, \theta) = \hat{F}(\hat{\rho}, \theta + \Delta\theta) \quad (10)$$

From this equation we conclude that the rotation over the angle $\Delta\theta$ is reduced to a shift over θ in log-polar space. Using the Fourier transforms of $\hat{F}(\hat{\rho}, \theta)$ and $\hat{G}(\hat{\rho}, \theta)$ we can from (10) obtain the formula (11):

$$F_2(w_{\hat{\rho}}, w_\theta) = \mathrm{e}^{-2i\pi(w_{\hat{\rho}} + \Delta\theta . w_\theta)} F_1(w_{\hat{\rho}}, w_\theta) \quad (11)$$

where $F_1(w_{\hat{\rho}}, w_\theta)$: Fourier transform of $\hat{F}(\hat{\rho}, \theta)$, $F_2(w_{\hat{\rho}}, w_\theta)$: Fourier Transform of $\hat{G}(\hat{\rho}, \theta)$.

Third step The normalized cross-power spectrum between F_1 and F_2 is defined as follows:

$$\hat{C}(u, v) = \frac{F_1 F_2^*}{||F_1 F_2^*||} = \mathrm{e}^{-2i\pi(w_{\hat{\rho}} + \Delta\theta . w_\theta)} \quad (12)$$

The inverse Fourier Transform is defined by:

$$IFT\left(\hat{C}(u, v)\right) = \delta(\hat{\rho}, \theta + \Delta\theta) \quad (13)$$

The Dirac delta function centered in $(0, -\Delta\theta)$ [20,21]. We note that the value of $\Delta\theta$ obtained by this technique is not very accurate. To improve this result, we propose to add another step.

4.1.2 Second step

In this step we use the differential technique from Lucas–Kanade [22] to find the accurate rotation between the two images, which was proven to be efficient and reliable. The Lucas–Kanade technique provides high estimation accuracy and low complexity, but it assumes that the displacements between images are small. Therefore, it is possible to use this technique to get high-accuracy rotation estimation.

Lucas–Kanade technique The basic of Lucas–Kanade method is defined as:

We denote an image by $f(x, y, t)$ and the velocity of an image pixel $P = [x, y]^{\mathrm{T}}$ is:

$$V = \left[v_x, v_y\right]^{\mathrm{T}} = \begin{bmatrix} \mathrm{d}x/\mathrm{d}t \\ \mathrm{d}y/\mathrm{d}t \end{bmatrix}$$

Assuming the pixel displacement is small between consecutive images. So, the intensity P keeps the same during $\mathrm{d}t$, i.e.,

$$f(x, y, t) = f(x + v_x \mathrm{d}t, y + v_y \mathrm{d}t, t + \mathrm{d}t) \quad (14)$$

The right side of Eq. (15) can be approximated by its first-order Taylor expansion.

$$f(x, y, t) = f(x, y, t) + \frac{\partial f}{\partial x} v_x \mathrm{d}t + \frac{\partial f}{\partial y} v_y \mathrm{d}t + \frac{\partial f}{\partial t} \mathrm{d}t + o\left(\mathrm{d}t^2\right) \quad (15)$$

This yields Eq. (16):

$$\frac{\partial f}{\partial x} v_x + \frac{\partial f}{\partial y} v_y + \frac{\partial f}{\partial t} = 0 \quad (16)$$

We call this equation optical flow constraint equation [22].

Equation (16) cannot be solved because of the existence of two unknowns in one equation, but if a small window is supposed to have the same velocity, the problem can have a solution. If the window size is N pixels $p_1, p_2, \ldots p_N$, the equation system is the one listed in (17).

$$\begin{aligned} &\frac{\partial f}{\partial x}(p_1) v_x + \frac{\partial f}{\partial y}(p_1) v_y + \frac{\partial f}{\partial t}(p_1) = 0 \\ &\frac{\partial f}{\partial x}(p_2) v_x + \frac{\partial f}{\partial y}(p_2) v_y + \frac{\partial f}{\partial t}(p_2) = 0 \\ &\qquad \ldots \\ &\frac{\partial f}{\partial x}(p_N) v_x + \frac{\partial f}{\partial y}(p_N) v_y + \frac{\partial f}{\partial t}(p_N) = 0 \end{aligned} \quad (17)$$

To solve this linear system we use least-squares method: Let:

$$A = \begin{pmatrix} \frac{\partial f}{\partial x}(p_1) & \frac{\partial f}{\partial y}(p_1) \\ \frac{\partial f}{\partial x}(p_2) & \frac{\partial f}{\partial y}(p_2) \\ \ldots & \\ \frac{\partial f}{\partial x}(p_N) & \frac{\partial f}{\partial y}(p_N) \end{pmatrix} \quad (18)$$

$$b = -\begin{pmatrix} \frac{\partial f}{\partial t}(p_1) \\ \frac{\partial f}{\partial t}(p_2) \\ \ldots \\ \frac{\partial f}{\partial t}(p_N) \end{pmatrix} \quad (19)$$

The velocity v_x and v_y can be computed by:

$$\begin{pmatrix} v_x \\ v_y \end{pmatrix} = \left(A^T A\right)^{-1} A^T b \quad (20)$$

Estimate the accurate rotation with Lucas–Kanade technique To obtain the accurate rotation with the Locus–Kanade described above, we use the following steps:

- Rotate the transformed image with the large angle detected in the first step;
- Get the magnitude Fourier Transform of the two images which exhibits the rotation, but not translation;

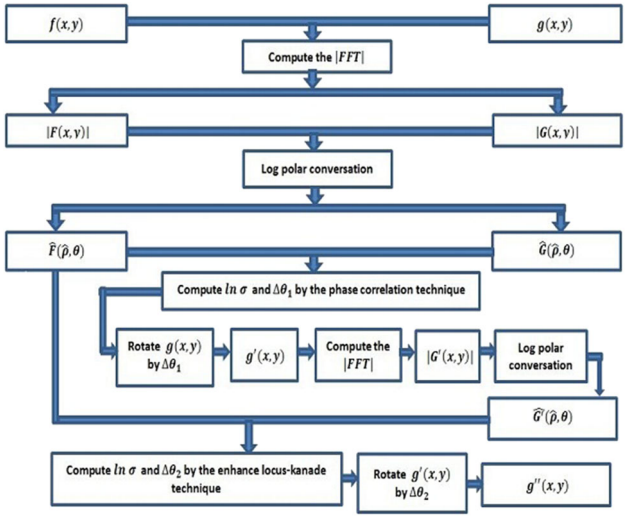

Fig. 1 The proposed algorithm for the accurate rotation estimation

- Convert the rotation into a translation by using the log-polar conversation;
- Detect interest points in reference image which refer to point features that represent two-dimensional intensity. The algorithm used to detect interest points is Harris corners detector which provides very accurate results [23];
- We extract a neighborhood (window of size nxn) centered at every corner;
- For each window, the Lucas–Kanade algorithm is applied. Consequently, we get many solutions to Eq. (20):

$$\left(\begin{pmatrix}\theta_{1x}\\ \rho_{1y}\end{pmatrix},\begin{pmatrix}\theta_{2x}\\ \rho_{2y}\end{pmatrix},\ldots\begin{pmatrix}\theta_{Nx}\\ \rho_{Ny}\end{pmatrix}\right) \tag{21}$$

where θ_x: the estimate angle, ρ_y: factor scale which equal to 1 in our case, N: number of corner points.

- Finally, the accurate solution is defined by:

$$\theta_x = \frac{1}{N}\sum_{i=1}^{N}\theta_{ix} \tag{22}$$

The block diagram of the rotation estimation is described in Fig. 1.

4.2 Shift estimation

4.2.1 First step

The goal of the first step of the proposed algorithm is to find the nearest integral pixel coordinates taking into account the required time and memory. In order to reach this object, we propose to down-sample FT of the source and reference images by down-sampling factors k_1 an k_2 along $\boldsymbol{u}$ and $\boldsymbol{v}$ directions, respectively, then apply the same procedure of phase correlation method described in Sect. 2.1. Therefore,

Table 1 The upper bounds of the down-sampling factors for an image of dimension 250 × 250, $\boldsymbol{k_1}$ and $\boldsymbol{k_2}$ the down-sampling factors along the x and y directions, respectively, $\boldsymbol{a}$ and $\boldsymbol{b}$ the ideal subpixel, $\hat{a}$ and $\hat{b}$ are the estimated subpixel shift

a	b	$\hat{a}$	$\hat{b}$	k_1	k_2
3.4879	6.1456	*3.4879*	*6.14560*	72	40
6.578	3.6579	*6.1578*	*3.65790*	40	68
17.2568	17.3658	*17.256*	*17.3658*	12	12
22.3568	22.7894	*22.356*	*22.7894*	8	80
3.4879	110.5698	*3.4879*	*110.569*	72	2
110.5698	4.3256	*110.56*	*4.32560*	2	58
17.2578	120.5674	*17.257*	*120.567*	14	2
3.4879	6.1456	**−2.1324**	**−8.1822**	100	60
6.1578	3.6579	**−3.2779**	**−3.6406**	52	110
17.2568	17.3658	**0.25350**	**−0.8724**	30	30
3.4879	110.5698	**0.87570**	**7.61570**	130	5
110.5698	4.3256	**23.7008**	**2.85320**	3	80
17.2578	120.5674	**−0.09380**	**16.9800**	45	5

the new version of the cross correlation described in (2) can be written as follows:

$$C^d\left(k_1u,k_2v\right) = \frac{F\left(k_1u,k_2v\right)G^*\left(k_1u,k_2v\right)}{\left|\left|F\left(k_1u,k_2v\right)G^*\left(k_1u,k_2v\right)\right|\right|} \tag{23}$$

The new dimension of the down-sampled cross spectrum c^d is $\frac{M}{k_1}\times\frac{N}{k_2}$. Consequently, the new complexity of this step is $o\left(\frac{MN\in}{k_1k_2}\right)$. Finally, the results of the registration are very satisfying if $a < \frac{M}{k_1}$ and $b < \frac{N}{k_2}$. Table 1 shows a demonstration of these upper bounds.

The discontinued edges in input images produce high frequencies which are totally wrong. Hence, the registration parameters estimated by Eq. (23) will be affected by these edges. Very common approaches used to reduce this effect by using window functions like Hanning window (18), Hamming window (19), and Blackman window (26).

$$w\left(x_1,x_2\right)_{\text{han}} = \left(0.5-0.5\cos\left(2\pi\left(\frac{x_1}{M}\right)\right)\right). \times\left(0.5-0.5\cos\left(2\pi\left(\frac{x_2}{N}\right)\right)\right) \tag{24}$$

$$w\left(x_1,x_2\right)_{ham} = \left(0.54-0.46\cos\left(2\pi\left(\frac{x_1}{M}\right)\right)\right). \times\left(0.54-0.46\cos\left(2\pi\left(\frac{x_2}{N}\right)\right)\right) \tag{25}$$

$$w\left(x_1,x_2\right)_{bla} = \left(0.42-0.5\cos\left(2\pi\left(\frac{x_1}{M}\right)\right)\right). \times\left(0.42-0.5\cos\left(2\pi\left(\frac{x_2}{N}\right)\right)\right) \tag{26}$$

N and M are the sizes of images.

Even though these window functions reduce the effect of discontinuity at image, they are not very effective in the

case where the two images contain the discontinued edges in the same regions. For this purpose, it is better to apply an improved version of 2D Hanning window defined by:

$$W(x_1, x_2) = \begin{cases} \alpha & w(x_1, x_2)_{\text{han}} > \alpha \\ w(x_1, x_2)_{\text{han}} & \text{otherwise} \end{cases} \quad (27)$$

By using this window, the effects of the wrong high frequencies can be removed in Eq. (23) and the image information concentrates in low frequency will not be changed. In Sect. 5, it will focus on demonstrating that the accuracy is more important when $\alpha = 0.9$.

4.2.2 Second step

The complexity time and memory requirements of the frequency domain approaches described in Sect. 3 are better than spatial domain approaches described in Sect. 2. The main drawback of these approaches is that we can achieve registration precision only if the shift parameters are very small, especially between 3 and 4 pixels and the phase angle data in (2) are 2 π wrapped. The first drawback is caused by aliased error; it is noted that this error can be minimized by using only frequencies that are free of aliasing. The second drawback can also be resolved by using ordinary smoothing filters to reduce the noise in the phase correlation. To do this, the direct Fourier method was chosen to refine a subpixel registration in the second step of the proposed algorithm by the following steps:

1. Compute cross correlation between source image f and reference image $\boldsymbol{g}$.
2. Apply a phase fringe filtering into phase angle of the cross correlation calculated.
3. Mask out high-frequency components of the cross-correlation matrix and only the lower-frequency part which is near to the origin is kept for the 2D fitting operation.
4. Write the linear equation $\frac{\boldsymbol{ua}}{\boldsymbol{M}} + \frac{\boldsymbol{vb}}{\boldsymbol{N}}$ describing a plane through the computed phase difference with unknown $\boldsymbol{a}$ and $\boldsymbol{b}$.
5. Find the shift parameters ($\boldsymbol{rowshift}, \boldsymbol{colshift}$) using the least-squares fitting method.

The phase fringe filtering [24] can be implemented as follow:

1. Find $\theta\,(u, v)$ the phase angle of the cross correlation.
2. Apply a smoothing filter to $\mathbf{sin}\,\boldsymbol{\theta}$ and $\mathbf{cos}\,\boldsymbol{\theta}$.
3. Conclude the filtered phase angle.

We note that the proposed algorithm is truly robust to change of intensity of the form:

$$i' = ai + b \quad (28)$$

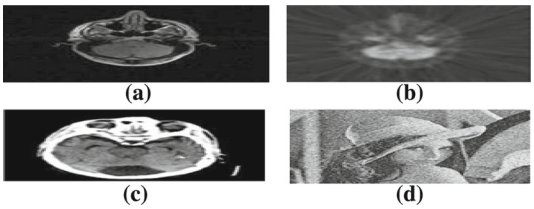

Fig. 2 The images used in algorithm performance testing. **a** Magnetic Resonance Imaging (MRI). **b** Positron Emission Tomography (PET) image. **c** Scanner image. **d** Lena image

The constants $\boldsymbol{a}$ and $\boldsymbol{b}$ change only the magnitude and the spectral coefficient at the origin, respectively, leaving the phase unchanged.

5 Simulations and results

In order to compare the accuracy, robustness against noise and time required of our approach with other algorithms, the algorithms were implemented in MATLAB, and all tests were performed on a 2.6 GHz Intel(R) Core(TM) 2 Duo processor, 32-bit operating system, 4 Gbytes (RAM).

5.1 The accuracy of the proposed algorithm

We applied the proposed algorithm to images represented in Fig. 2. The experiments consist on generating hundred target images by translating and rotating the reference image into known displacement images. For each algorithm, the estimated registration parameters were compared to the true parameters to determine the accuracy of the registration. The registration error is computed as follows:

$$E = \frac{1}{2}\left(|\hat{a} - a| + \left|\hat{b} - b\right|\right) \quad (29)$$

The improved window function was applied to the input images in the frequency domain, then the registration error of the proposed algorithm was evaluated for different values of α [α is described in Eq. (27)]. Figure 3 shows the results of this evaluation. From this figure, we conclude that the improved window has a good convergence error when $\alpha = 0.9$ compared to Hanning window.

To test the performance of our algorithm, two different subpixel registration algorithms proposed by Guizar-Sicairos et al. [14] described in Sect. 2, and by Amr Yousef et al. [25] based on up-sampled cross correlation of down-sampled Fourier transform, we refer to it as Down-sampled Single-Step DFT approach (DSSDFT). For different image dimensions, the down-sampling factors in the first step of the proposed approach and the DSSDFT approach were selected to be $\frac{\boldsymbol{M}}{\mathbf{16}}$ and $\frac{\boldsymbol{N}}{\mathbf{16}}$. Figure 4 shows the registration error of the tree algorithms applied on hundred shifted images generated by translating the reference image by a known displacement,

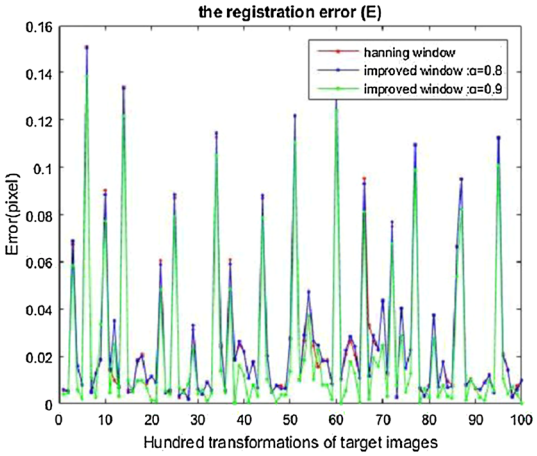

Fig. 3 The registration error of hundred transformations for Hanning window and improved window with $\alpha = 0.8$ and $\alpha = 0.9$ (improved window parameter)

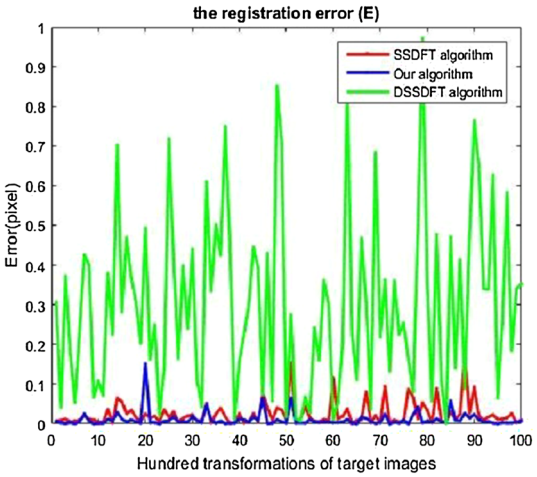

Fig. 4 The registration error of SSDFT, DSSFT and the proposed algorithm

where the X axis represents the hundred displacements and Y axis represents the registration error. As a conclusion, the proposed algorithm provided excellent results compared to other algorithms.

Table 1 indicates the upper bound of the down-sampling factors. This upper bound has been mentioned in Sect. 4. All values of the down-sampling factors were tested. In the table, the italics values indicated the satisfied upper bounds and the bold italics for the wrong bounds. The performance of the proposed algorithm is very satisfied when the upper bounds are respected ($a < \frac{M}{k_1}$ and $b < \frac{N}{k_2}$).

Tables 2 and 3 show the results of parameters of translation and rotation of our algorithm and Vandewalle [16] method, respectively. From these tables we conclude that our algorithm is good for the large and small rotations and translations, but the P. Vandewalle method is good only for small transformations.

Table 2 Parameters estimation (translation and rotation) by our algorithm

Transformations between images		Parameters estimation By our algorithm	
Translation (pixels)	Rotation (degree)	Translation (pixels)	Rotation (degree)
(0.5647, 1.8974)	1.3578	(0.5638, 1.9071)	1.3608
(0.3365, 0.4789)	25.3578	(0.3301, 0.5009)	25.3173
(35.7895, 10.324)	0.3345	(35.779, 10.331)	0.3334
(40.125, 40.6984)	42.2564	(40.2035, 40.7176)	42.2680

Table 3 Parameters estimation (translation and rotation) by Vandewalle method

Transformations between images		Parameters estimation by Vandewalle method	
Translation (pixels)	Rotation (degree)	Translation (pixels)	Rotation (degree)
(0.5647, 1.8974)	1.3578	0.5214, 1.9864	1.8905
(0.3365, 0.4789)	25.3578	10.61, 2.4709	1.7852
(35.7895, 10.3245)	0.3345	12.7468, 40.4789	0.3378
(40.1235, 40.69854)	42.2564	1.8746, 6.7825	16.3325

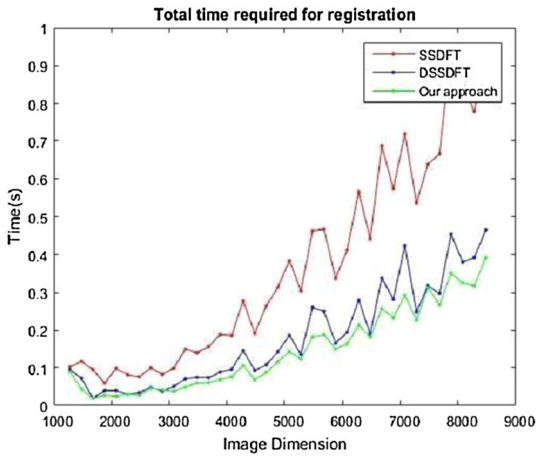

Fig. 5 Comparison of the computation times required between the SSDFT, DSSDFT and the proposed algorithm

5.2 The time required by the proposed algorithm

The dimension of the reference images that we used is from 250×250 up to 1000×1000. These images are corrupted by additive zero-mean circular complex Gaussian noise and translated by $(a, b) = (12.369874, 20.836974)$ pixels to create shifted images. Figure 5 shows a comparison of the computation times required between the SSDFT, DSSDFT and the proposed algorithm. It can be seen that our approach is faster than the other approaches. For 250×250 images, the computation times took 0.0437 s by our algorithm, 0.0452 by DSSDFT, and 0.0758 by SSDFT. This result is very impor-

Table 4 The time required to register images of dimensions 250 × 250 by changing the required subpixel accuracy

Subpixel accuracy	Proposed approach (s)	DSSDFT (s)	SSDFT (s)
0.1	0.0336	0.0402	0.0720
0.01	0.0415	0.0552	0.0894
0.001	0.0496	0.0651	1.942

tant, especially when we would like to get the real-time image registration. To verify the results obtained in Fig. 5, the Table 4 shows the time required to register images of 250 × 250 dimensions by changing the required subpixel accuracy. The subpixel accuracy of the proposed algorithm is better than other algorithms. In addition, we can state a great reduction in computation time.

6 Conclusion

This paper presents a new algorithm which estimates the accurate rotation and subpixel translation. For the rotation, we propose to use Fourier Mellin Transform combined with the phase correlation technique in the first step. In the second step, an enhance Lucas–Kanade was proposed to estimate the accurate rotation. For the shift translation, the technique that we describe in this paper consists of six steps. First, refine the initial translation parameters, which refer to the maximum point on the cross-correlation surface and transform the Reference Image with the estimated parameters. Second, calculate the new cross-correlation surface, then apply a phase fringe filter to reduce the noise in the phase correlation. Then, high-frequency components of the cross-correlation matrix are masked out and only the lower-frequency part which is near to the origin is kept for the 2D fitting operation. Finally, find the shift parameters using the least-squares fitting method. This approach offers an improvement in terms of both computation time and memory requirements comparably with some other algorithms.

References

1. Tian, Q., HUHNS, N.M.: Algorithms for subpixel registration. Comput. Vis. Graph. Image Process. **35**, 220–233 (1986)
2. Feng, S., et al.: A coarse-to-fine subpixel registration method to recover local perspective deformation in the application of image super-resolution. IEEE Trans. Image Process. **1**, 53–66 (2012)
3. Flusser, J., Zitova, B.: Image registration methods: a survey. Image Vis. Comput. **21**(11), 977–1000 (2003)
4. Jenkinson, M., Smith, S.: Aglobal optimisation method for robust affine registration of brain images. Med. Image Anal. **5**(2), 143–156 (2001)
5. Davatzikos, C.: Spatial transformation and registration o fbrain images using elastically deformable models. Comput. Vis. Image Underst. **66**(2), 207–222 (1997)
6. Gallea, R., et al.: Three-dimensional fuzzy kernel regression framework for registration of medical volume data. Pattern Recognit. **46**(11), 3000–3016 (2013)
7. Alpert, N.M., et al.: Improved methods for imageregistration. NeuroImage **3**, 10–18 (1996)
8. Brown, L.G.: A survey of image registration techniques. ACM Comput. Surv. **24**(4), 325–376 (1992)
9. Roche, A. et al.: The correlation ratio as a new similarity measure for multimodal image registration. In: Medical Image Computing and Computer-Assisted Interventation, pp. 1115–1124 (1998)
10. Viola, P.: Alignment by maximisation of mutual information. Int. J. Comput. Vis. **24**(2), 147–154 (1997)
11. Kuglin, C.D., Hines, D.C.: The phase correlation image alignment method. In: Proceeding of IEEE International Conference on Cybernetics and Society, New York, NY, USA, [s.n.], pp. 163–165 (1975)
12. Foroosh, H., Zerubia, J.B., Marc, B.: Extension of phase correlation to subpixel registration. IEEE Trans. Image Process. **11**(3), 188–200 (2002)
13. Takita, K., et al.: High-accuracy subpixel image registration based on phase-only correlation. IEICE Trans. Fundam. **E86A**(8), 1925–1934 (2003)
14. Guizar-Sicairos, M., Thurman, S.T., Fienup, J.R.: Efficient subpixel image registration algorithms. Opt. Lett. **33**(2), 156–158 (2008)
15. Kim, S.P., Su, W.-Y.: Subpixel accuracy image registration by spectrum cancellation. In: Proceedings of the ICASSP, pp. 153–156 (1993)
16. Vandewalle, P., Susstrunk, S., Vetterli, M.: A frequency domain approach to registration of aliased images with application to super-resolution. EURASIP J. Appl. Signal Process. **2006**, 233–233 (2006)
17. Stone, H.S., et al.: A fast direct Fourier-based algorithm for subpixel registration of images. IEEE Trans. Geosci. Remote Sens. **39**(10), 2235–2243 (2001)
18. Foroosh, H., Balci, M.: Subpixel registration directly from the phase difference. EURASIP J. Appl. Signal Process. **2006**, 1–11 (2006)
19. Tsay, R.Y., Huang, T.S.: Multiframe image restoration and registration. Adv. Comput. Vis. Image Process. **1**, 317–339 (1984)
20. Reddy, B.S., Chatterji, B.N.: An FFT-based technique for translation, rotation, and scale-invariant image registration. IEEE Trans. Image Process. **5**(8), 1266–1270 (1996)
21. Marcel, B., Briot, M., Murrieta, R.: Calcul de translation et rotation par la transformation de Fourier. Traitement du signal **14**(2), 135–149 (1997)
22. Bruce, D.L., Takeo, K.: An iterative image registration technique with an application to stereo vision. In: Proceedings of the 7th International Joint Conference on Artificial Intelligence, pp. 674–679 (1981)
23. Mohanna, F., Mokhtarian, F.: Performance evaluation of corner detection algorithms under similarity and affine transforms. In: Cootes, T., Taylor, C. (eds.) Proceedings of the British Machine Conference, pp. 37.1–37.10. BMVA Press, September 2001. doi:10.5244/C.15.37
24. Wang, F., Prinet, V., Sonede, M.: A vector filtering technique for sar interferometric phase image. Institute of Automation, Chinese Academy of Sciences, Beijing, China. http://www.kesala.net/pub/Confs/2001/wang01b-filtering.pdf (2001)
25. Amr, Y., Li, J., Ataul, K.M.: High-speed image registration algorithm with subpixel accuracy. IEEE Signal Process. Lett. **22** (10), 1796–1800 (2015)